This article has been accepted for publication in a future issue of this journal, but has not been fully edited. Content may change prior to final publication. Citation information: DOI 10.1109/LAWP.2015.2428436, IEEE Antennas and Wireless Propagation Letters

Ultra-Wideband Planar Gaussian Tapered Rhombic Antenna for Short Pulse Applications

Mei Yang, *Student member, IEEE*, Xiaoxing Yin, *Member, IEEE*, Yufu Li, *Student member, IEEE*, and Leilei Liu, *Member, IEEE*

***Abstract*—An ultra-wideband planar rhombic antenna with Gaussian tapered profile is proposed for short pulse applications. Compared to a conventional linear rhombic antenna, the proposed antenna has a smooth Gaussian tapered edge, which can diminish the reflected pulse signal and thus can enlarge the bandwidth significantly. The proposed planar Gaussian tapered rhombic antenna was fabricated and its performance both in frequency domain and in time domain was investigated. Good agreements between the simulated and the measured results have been observed. Both of the simulated and the measured results show that the proposed antenna is featured by broad bandwidth, low cross polarization levels, and suitability for short pulse applications.**

***Index Terms*—Gaussian tapered rhombic antenna, planar antenna, short pulse, traveling wave, ultra-wideband.**

I. Introduction

Rhombic antenna is a typical traveling wave antenna, which is widely used because of its wide bandwidth and the simplicity (linear profile) of construction [1]. Considering its travelling wave feature and wideband performance, rhombic antenna is a good choice for short pulse applications, such as ground penetrating radar, high speed imaging, and so on. However, the sudden turns in the feeding section and in the middle of the rhombic antenna produce large reflection, which deteriorates the traveling wave feature of the antenna and lays severe constraints on the antenna bandwidth.

Vee antenna, usually treated as half of a rhombic antenna, is also a travelling antenna. Diverse tapered profiles, such as the common exponential profile [2] and the subsequently emerged Fermi [3], hyperbolic [4], elliptic [5], half-Gaussian profile [6], and other optimized profiles [6-8], are proposed to implement planar variations of Vee antennas to improve the antenna performance. However, there is little literature on the planar rhombic antennas and on the optimization of the profiles of the planar rhombic antenna. And mechanically employing the tapered profile of a Vee antenna on the four arms of a planar rhombic antenna may also lead to enormous reflection.

In this letter, an ultra-wideband planar Gaussian tapered rhombic antenna is proposed. The proposed tapered profile, different from the half-Gaussian profile reported in [6], tapers gradually in a Gaussian curve in the diverging segment at first and then presenting a smooth transition to the converging segment tapered in another Gaussian curve. The proposed Gaussian tapered profile is favorable for diminishing reflected pulse signals caused by sudden bents and thus can enlarge the bandwidth significantly. The prototype of the planar Gaussian tapered rhombic antenna was fabricated and measured. The simulated and the measured results, both in frequency domain and in time domain, show that the proposed antenna is featured by broad bandwidth, low cross polarization levels, and suitability for short pulse applications.

II. Antenna Configuration and Analysis

The geometry of the proposed Gaussian tapered rhombic antenna is shown in Fig. 1 (a). The two fins of the proposed rhombic antenna are etched on opposite sides of a substrate, therefore the proposed antenna can be easily fed by a coaxial connector. The proposed tapered profile diverges gradually in the region of $-l_1 \le z \le 0$ and converges in the region of $0 \le z \le l_2$ in accordance with the Gaussian functions expressed as follows

$$x(z) = \begin{cases} a \cdot \exp(-4\pi(\frac{z}{\tau_1})^2), & -l_1 \le z \le 0 \\ a \cdot \exp(-4\pi(\frac{z}{\tau_2})^2), & 0 \le z \le l_2 \end{cases} . \quad (1)$$

where a determines the maximum of the Gaussian curves, and τ_1 and τ_2 indicate the width of the Gaussian profiles. A resistor with value of R is utilized to bridge the two converging antenna fins at the terminal point C.

For comparison, a planar conventional rhombic antenna with the same dimensions is also designed, as depicted in Fig. 1 (b). For the conventional rhombic antenna, the reflected pulse signals aroused at the feeding point A′ and the middle turn point B′ severely limit the impedance bandwidth. The Gaussian tapered profile of the proposed antenna has a smaller variation rate at the feeding point A compared to the conventional rhombic profile (at apex A′). Additionally, the derivative of the Gaussian profile at the middle turn point B is zero, which indicates a smooth transition from the diverging segment to the converging segment.

The proposed Gaussian tapered rhombic antenna is modeled

This work was supported by National Natural Science Foundation of China under Grant No. 61427801, and in part by Specialized Research Fund for the Doctoral Program of Higher Education under Grant No. 20133223120005.

Mei Yang, Xiaoxing Yin, and Yufu Li are with the State Key Laboratory of Millimeter Waves, Southeast University, Nanjing 210096, China (e-mail: 101010074@seu.edu.cn).

Leilei Liu is with the School of Electronic Science and Engineering, Nanjing University of Posts and Telecommunications, Nanjing 210003, China.

This article has been accepted for publication in a future issue of this journal, but has not been fully edited. Content may change prior to final publication. Citation information: DOI 10.1109/LAWP.2015.2428436, IEEE Antennas and Wireless Propagation Letters

in CST MWS and time domain solver is used to obtain the antenna performance. In this design, Rogers 4003C with a relative permittivity of 3.55 and a thickness of 0.813 mm is used as the substrate. For accuracy, the SMA connector is also included in the simulation. The Gaussian pulse with a -10 dB bandwidth from DC to 20 GHz is utilized to excite the proposed antenna and is expressed as

$$G(t)=e^{-\frac{4\pi(t-t_0)^2}{\tau^2}} \quad (2)$$

where t_0 equals to 0.08885 ns and τ is 0.086 ns.

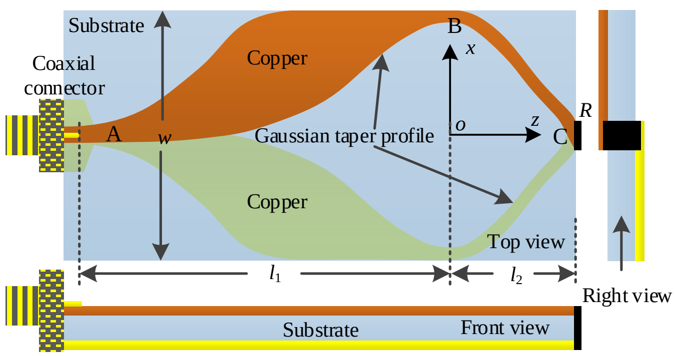

(a)

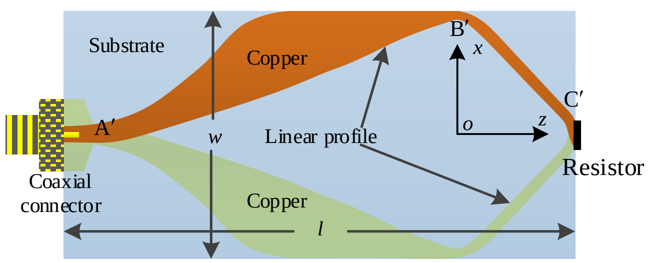

(b)

Fig. 1. Geometry of the antennas. (a) The proposed Gaussian tapered rhombic antenna. (b) The planar conventional rhombic antenna.

The effect of the terminating resistor on the reflected pulse signal is shown in Fig. 2. It can be found that the reflected pulse is greatly decreased when the resistor is 200 Ohms compared to other smaller or larger values. The final parameters of the Gaussian profile antenna, after optimization in CST MWS, are given in Table I.

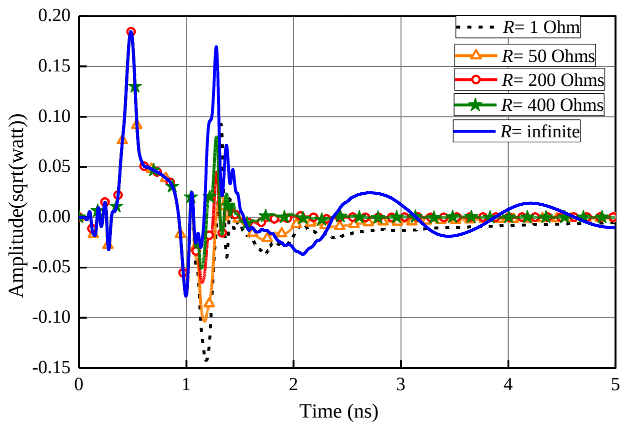

Fig. 2. The reflected pulse signals with different terminating resistors.

TABLE I
PARAMETERS OF THE PROPOSED ANTENNA

l	w	l_1	l_2	a	τ_1	τ_2	R
110 mm	54 mm	80 mm	25 mm	25	120	42	200 Ohms

The reflection coefficient $|S_{11}|$ and the reflected pulse b_{11} of the proposed antenna are shown in Fig. 3. For comparison, the performance of the conventional rhombic antenna with the same dimensions is also depicted in Fig. 3. From the appearance time of the peaks of the reflected pulse signals, it can be concluded that the reflection in the proposed antenna is mainly produced by the discontinuity at apexes A and B, and the reflection in the conventional rhombic antenna mainly occurs at apexes A′ and B′. Meanwhile, it can be found that the peak value of the reflected pulse signal for the proposed Gaussian tapered rhombic antenna at A is about half of that for the conventional rhombic antenna at A′. Consequently, the reflection coefficient for the proposed antenna decreases about 6 dB in the frequency range from 1.48 GHz to 12 GHz compared to that of the conventional rhombic antenna, as shown in Fig. 3. Correspondingly, the lower limit operating frequency is extended from 7.7 GHz to 1.48 GHz.

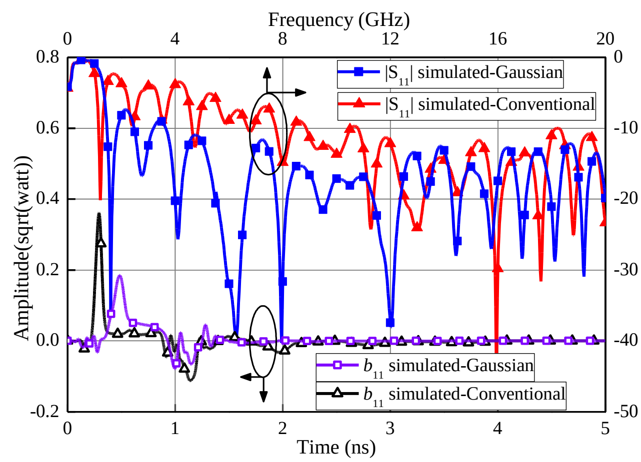

Fig. 3. The reflected pulse signals and the reflection coefficients for the Gaussian tapered rhombic antenna and the conventional rhombic antenna.

III. SIMULATED AND EXPERIMENTAL RESULTS

In order to characterize the radiation performance of the proposed antenna, the prototype, whose parameters are shown in Table I, was fabricated and is shown in Fig. 4 (a). For comparison, a planar conventional rhombic antenna was also fabricated using the same substrate and is depicted in Fig. 4 (b).

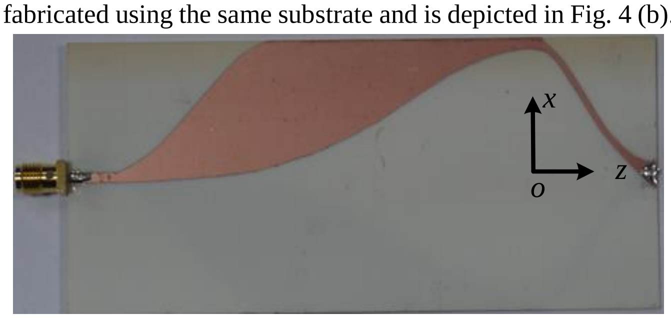

(a)

This article has been accepted for publication in a future issue of this journal, but has not been fully edited. Content may change prior to final publication. Citation information: DOI 10.1109/LAWP.2015.2428436, IEEE Antennas and Wireless Propagation Letters

(b)

Fig. 4. The fabricated antennas. (a) The Gaussian tapered rhombic antenna. (b) The conventional rhombic antenna.

A. Reflection Coefficients and Reflected Pulse Signals

The reflection coefficients of the fabricated antennas were measured using a calibrated Agilent vector network analyzer N5230A. The measured reflected pulse signals $b_{11}(t)$ can be expressed as

$$b_{11}(t) = \mathrm{IFFT}[\mathrm{G}(f) \cdot S_{11}(f)] \quad (3)$$

where $S_{11}(f)$ represents the measured scattering parameters of the fabricated antennas and $G(f)$ is the spectrum of the Gaussian pulse given in (2).

Comparisons between the simulated and measured reflected pulse signals b_{11} at the antenna ports and $|S_{11}|$ are shown in Fig. 5 (a) and Fig. 5 (b) respectively. A good consistency has been observed between the simulated and the measured results. Due to the Gaussian tapered profile, the reflected pulse signal of the proposed antenna has been significantly diminished compared to that of the conventional rhombic antenna, which leads to the enlargement of the impedance bandwidth. As shown in Fig. 5 (b), the proposed antenna has an ultra-wideband frequency band ranging from 1.48 GHz to 20 GHz while that for the conventional rhombic antenna is 7.7 GHz to 20 GHz.

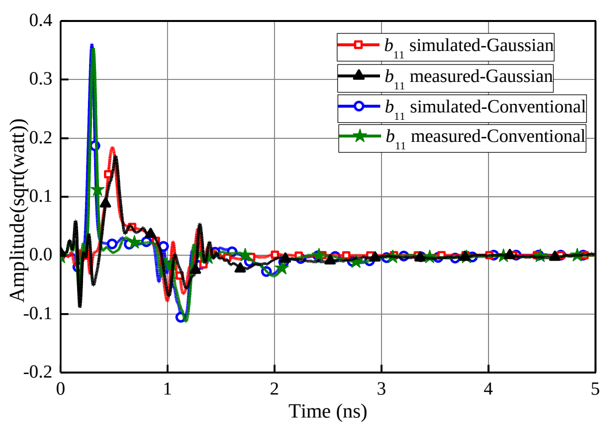

(a)

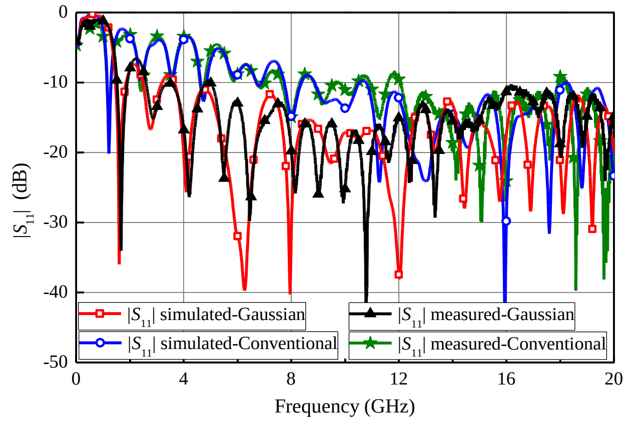

(b)

Fig. 5. The simulated and measured reflected pulse signals and the reflection coefficients for the two rhombic antennas. (a) The reflected pulse signals. (b) The reflection coefficients.

B. Patterns, Gain and Cross Polarization Level

The radiation performance of the proposed antenna was measured in anechoic chamber. Considering the large bandwidth of the proposed antenna, the patterns at 6 GHz, 10 GHz, 14 GHz, and 18 GHz were measured and are shown in Fig. 6, along with the corresponding simulated results to characterize the radiation performance. The measured and simulated radiation patterns agree very well. It is founded that the proposed antenna has a directional radiation patterns and the main direction is along the *z* axis. The sidelobe level of the proposed antenna is roughly -10dB in frequency band below 14 GHz and is about -5 dB at 18GHz.

The gain and the cross polarization level along the *z* direction for the proposed antenna are shown in Fig. 7. It can be found that the measured and the simulated gain agree very well across the involved frequency range, and the gain is quite flat from 6 GHz to 18 GHz. The cross polarization level of the proposed antenna is quite low, and it is lower than -20 dB from 2 GHz to 12 GHz based on the measured result.

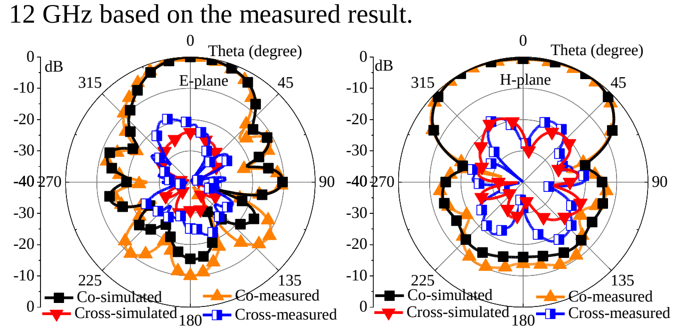

(a)

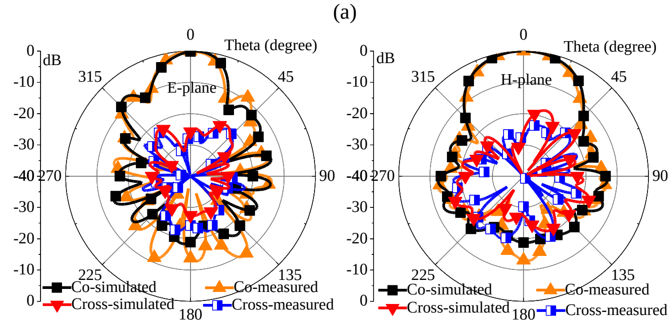

(b)

This article has been accepted for publication in a future issue of this journal, but has not been fully edited. Content may change prior to final publication. Citation information: DOI 10.1109/LAWP.2015.2428436, IEEE Antennas and Wireless Propagation Letters

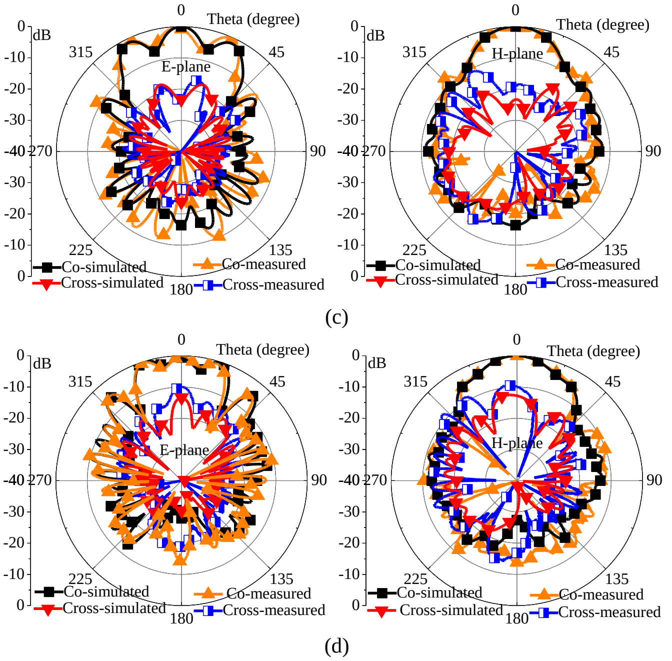

Fig. 6. The E-plane (*xoz* plane, left) and H-plane (*yoz* plane, right) patterns for the proposed antenna. (a) 6 GHz. (b) 10 GHz. (c) 14 GHz. (d) 18 GHz.

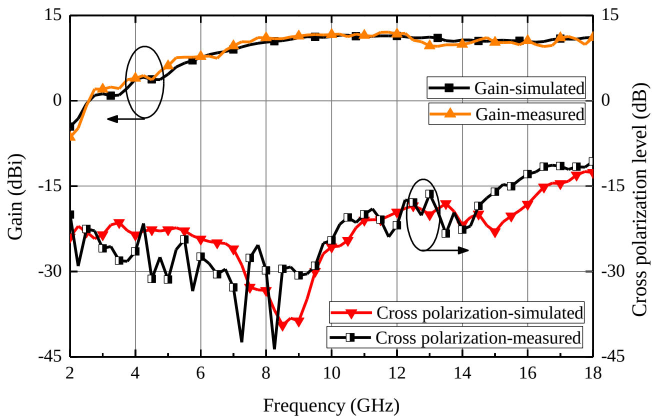

Fig. 7. The gain and the cross polarization level of the proposed antenna.

C. Transmission Performance in Time Domain

Two identical proposed antennas were placed 1.3 meters apart along the main radiation direction in the anechoic chamber and the transmission coefficients ($S_{21}(f)$) under the co-polarization and the cross polarization conditions were measured by using vector network analyzer. Being similar to (3), the corresponding transmission signal $b_{21}(t)$ in time domain is determined by the spectrum of the Gaussian pulse $G(f)$ and the measured $S_{21}(f)$, which can be expressed as

$$b_{21}(t) = \text{IFFT}[\text{G}(f) \cdot S_{21}(f)]. \qquad (4)$$

Fig. 8 gives the measured transmission signals $b_{21}(t)$ of the two identical antennas positioned in co-polarization and in cross polarization respectively. According to the pulse signal obtained in co-polarization condition, the ringing level is lower than -19.7 dB [9]. The system fidelity factor for the proposed antennas is 0.71 [10]. Therefore, both of the small tailing effect and the weak distortion demonstrate that the proposed Gaussian tapered rhombic antenna is suitable for short pulse applications.

In addition, the maximal amplitude of the co-polarization short pulse signal for the proposed antenna is 20 dB higher than that of the cross polarization situation. Both the cross polarization levels shown in frequency domain and time domain indicate the well polarization purity performance of the proposed antenna.

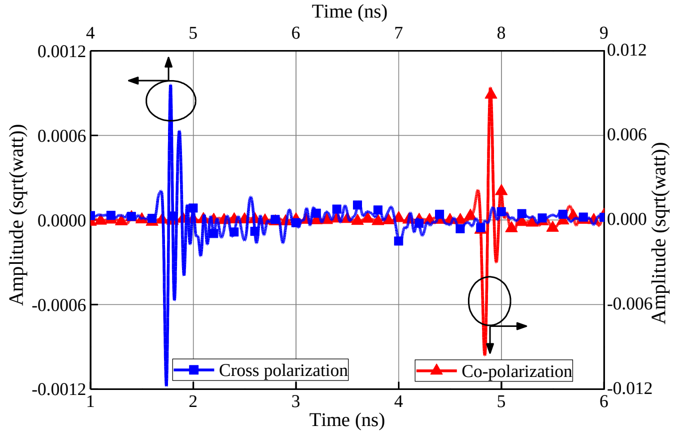

Fig. 8. The transmission short pulse signals between two proposed antennas.

IV. Conclusion

In this letter, an ultra-wideband planar Gaussian tapered rhombic antenna is proposed. The Gaussian tapered profile diminishes the reflected pulse signal and therefore enlarges the bandwidth significantly compared to the conventional rhombic profile. The simulated and measured results, both in frequency domain and time domain, show that the proposed antenna is featured by broad bandwidth, low cross polarization levels, and suitability for short pulse applications.

References

[1] C. H. Walters, *Traveling Wave Antennas*. New York, USA: Dover, 1970, pp. 319-321.

[2] P. J. Gibson, "The Vivaldi aerial," in *Proc. EuMC*, Brighton, U.K., 1979, pp. 101-105.

[3] S. Sugawara, Y. Maita, K. Adachi, K. Mori, and K. Mizuno, "A mm-wave tapered slot antenna with improved radiation pattern," in *IEEE-IMS*, Denver, CO, 1997, pp. 959-962.

[4] H. Nakajima, T. Kosugi, and T. Enoki, "Hyperbolic tangent tapered slot antenna," *Electron. Lett.*, vol. 46, no. 21, pp. 1422-1424, 2010.

[5] X. Qing, Z. N. Chen, and M. Y. W. Chia, "Dual elliptically tapered antipodal slot antenna loaded by curved terminations for ultrawideband applications," *Radio Science*, vol. 41, no. 6, 2006.

[6] K. Ebnabbasi, D. Busuioc, R. Birken, and M. Wang, "Taper design of Vivaldi and co-planar tapered slot antenna (TSA) by Chebyshev transformer," *IEEE Trans. Antennas Propag*., vol. 60, no. 5, pp. 2252-2259, May. 2012.

[7] H. Oraizi and S. Jam, "Optimum design of tapered slot antenna profile," *IEEE Trans. Antennas Propag*., vol. 51, no. 8, pp. 1987–1995, Aug. 2003.

[8] K. Ebnabbasi, S. Sczyslo, and M. Mohebbi, "UWB Performance of coplanar tapered slot antennas," *IEEE Antennas Wireless Propag. Lett*., vol. 12, pp. 749-752, 2013.

[9] H. Jeongwoo, and C. Nguyen, "A new ultra-wideband, ultra-short monocycle pulse generator with reduced ringing," *IEEE Microw. Wireless Compon. Lett*., vol.12, no.6, pp.206-208, Jun. 2002.

[10] G. Quintero, J. F. Zurcher, and A. K. Skrivervik, "System fidelity factor: a new method for comparing UWB antennas," *IEEE Trans. Antennas Propagat.*, vol. 59, no. 7, pp. 2502-2512, Jul. 2011.